

# Synthesis, Structure, and Optical Limiting Properties of an Axial Substituted Bis(8-oxide quinoline)zirconium Phthalocyanine<sup>①</sup>

YOU Ming-Hua<sup>a, b</sup> FANG Xin<sup>b</sup> LIN Mei-Jin<sup>b②</sup>

<sup>a</sup>(College of Zhicheng, Fuzhou University, Fuzhou 350002, China)

<sup>b</sup>(College of Chemistry, Fuzhou University, Fuzhou 350116, China)

**ABSTRACT** A novel bis(8-oxide quinoline)zirconium phthalocyanine [(OQ)<sub>2</sub>ZrPc] with two 8-oxide quinolone anions at the same axial positions has been successfully synthesized and its chemical structure has been assigned by the <sup>1</sup>H NMR, MS and two-dimensional correlation infrared (2D-IR) spectroscopy as well as by single-crystal X-ray structural analysis. It possessed a moderately effective nonlinear absorption coefficient  $\beta_{eff}$  of  $6.69 \times 10^{-14}$  cm/GW at 532 nm in DMF solution, implying it is a promising candidate for nonlinear optical materials.

**Keywords:** phthalocyanines, zirconium complex, axial substitution, single-crystal structure, optical limiting properties; **DOI:** 10.14102/j.cnki.0254-5861.2011-2132

## 1 INTRODUCTION

Organic optical limiting materials are an emerging class of active organic materials whose transmission is high when they are illuminated by low-intensity light but low when exposed to intense laser radiation<sup>[1-3]</sup>. Because of their potential applications in the protection of optical sensors from high-intensity laser beams, the search for better organic optical limiting materials has become increasingly interesting. Some criteria necessary for large, positive nonlinear absorption have been summarized, including a large excited state cross section, and a large difference between the ground and excited state absorption cross sections. A variety of organic materials have been found to fulfill these conditions in the visible region<sup>[4-6]</sup>, for example, fullerenes, porphyrins and asymmetrical conjugated systems<sup>[7-9]</sup>.

Phthalocyanines (Pcs) is an attractive class of

porphyrin homologues with larger  $\pi$ -electron conjugations, which have been demonstrated to be promising organic optical limiting materials<sup>[10-13]</sup>. However, comparison of nonlinear absorption coefficients  $\beta$  for Pcs with and without axial substituents indicates that those with axial substituents, *e.g.* PcVO, PcTiO, PcAlF, PcGaCl, PcInCl, have large nonlinear absorption coefficients<sup>[14-18]</sup>. The main reason for this is that the axial substitution in phthalocyanine (Pc) complexes has provoked relevant changes: (1) modification of the electronic structures of the Pc molecules by altering the  $\pi$ -electronic distribution; (2) introduction of a dipole moment perpendicular to the Pc planes; (3) incorporation of new steric effects that alter the spatial relationships between neighboring molecules, thus altering the magnitude of the intermolecular interactions<sup>[19]</sup>. As a versatile class of the axial substituted Pcs, zirconium (IV, Zr) Pcs meet the

Received 15 July 2018; accepted 13 August 2018 (CCDC 1848514 for (OQ)<sub>2</sub>ZrPc)

① This work was supported by the Natural Science Foundation of Fujian Province (2018J01431 and 2018J01690) as well as Research Foundation of Education Bureau of Fujian Province (JT180813)

② Corresponding author. Prof. Lin Mei-Jin, for the research interests, see homepage: <http://supramol.fzu.edu.cn>; E-mail: [meijin\\_lin@fzu.edu.cn](mailto:meijin_lin@fzu.edu.cn)

above-mentioned criteria well. More importantly, due to the unique coordination patterns of  $Zr^{4+}$  cations, up to four coordination sites are free for further coordination at the same axial position of the ZrPcs, and thus much larger room is left to regulate their optical limiting properties by the axial substituents in comparison with the reported Pcs with only one coordination site at the axial position. To our surprise, no related report is available.

To compensate this leak, herein we report a novel axially substituted ZrPc with two 8-oxide quinolone anions at the same axial positions,  $(OQ)_2ZrPc$ , and its chemical structure has been characterized by the  $^1H$  NMR, mass spectral (MS) and two-dimensional correlation infrared ( $2D$ -IR) spectroscopy as well as by single-crystal X-ray structural analysis. Owing to the introduction of two 8-oxide quinolone anions at the axial positions, the supramolecular interactions between the neighboring Pc molecules are remarkably weakened, particularly in solutions. The nonlinear optical properties of this unique complex have been studied by the open aperture  $Z$ -scan and normalized transmittance, which showed a moderately effective nonlinear absorption coefficient  $\beta_{eff}$  of  $6.69 \times 10^{-14}$  cm/GW but a high transmittance of 78% at 532 nm in DMF solution, implying it is a promising candidate for nonlinear optical materials.

## 2 EXPERIMENTAL

### 2.1 Materials and measurements

Phtalonitrile (97%), 2-methylnaphthalene, 1-chloronaphthalene, 8-hydroxyquinoline (HOQ), and zirconium chloride ( $ZrCl_4$ ) were obtained from commercial suppliers. All chemicals and reagents were used as received unless otherwise stated. Nuclear magnetic resonance (NMR) spectra were recorded on a Bruker Avance 400 spectrometer with working frequencies of 400 MHz. Chemical shifts are given in parts per million (ppm) and referred to TMS as internal standard.  $^1H$  coupling constants  $J$  are given in Hertz (Hz). Mass spectrum was recorded on a Deca xp MAX ion trap mass spectrometer.

Powder X-ray diffraction (PXRD) intensities were recorded on a Rigaku Mini Flex-II X-Ray diffractometer. The UV/Vis spectrum was recorded on a Perkins Elmer Lambda 900 spectrometer equipped with a PTP-1 Peltier temperature controller. The single-crystal diffraction data were collected on a Rigaku Saturn 724 CCD area detector diffractometer and the  $2D$ -IR correlation spectra were recorded on a Perkin-Elmer spectrum 2000 FT-IR spectrometer using KBr pellets, with the increasing temperature from 50 to 120 °C at an interval of 10 °C. The temperature variation was controlled by a portable programmable temperature controller (Model 50-886, Love Control Corporation). Two-dimensional IR correlation spectra were obtained by the treatment of a series of dynamic spectra with  $2D$ -IR correlation analysis software provided by Tsinghua University.

### 2.2 Synthesis of $(OQ)_2ZrPc$

To a 1-chloronaphthalene (14 mL) solution of phtalonitrile (6.41 g, 50.0mmol) and 2-methylnaphthalene (1.77 g, 12.5mmol), 2.92 g  $ZrCl_4$  (12.5 mmol) was added and the mixture was reacted under 220 °C for about 5 h. After the solution cooled down to 50 °C, the solid separated out from the solution was collected by filtration and then washed with benzene (~500 mL) and methanol (~500 mL) repeatedly until the color of the washing solvent changed to light blue. After being dried under 80 °C, dark blue powder (2.37 g, 65.4%) was obtained as  $Cl_2ZrPc$ . The sample was used without further characterizations. Around 0.02 g blue solid obtained (0.069 mmol) and 0.39 g HOQ (2.69 mmol) were dissolved in tetrahydrofuran (THF, 20 mL) and stirred for 6 hours under room temperature, and then the solution was filtrated. After the THF solvent was slowly evaporated under room temperature, dark blue small single crystals appeared in the solution. After filtration and drying under 40 °C, 0.022 g crystalline  $(OQ)_2ZrPc$  (62.7%) was obtained.  $^1H$  NMR (400 MHz,  $CDCl_3$ )  $\delta$ , ppm: 9.39~9.36 (q, 4H), 9.14~9.11 (q, 4H), 8.31~8.29 (q, 4H), 8.05~8.03 (q, 4H), 7.47 (d, 2H), 7.23 (t,

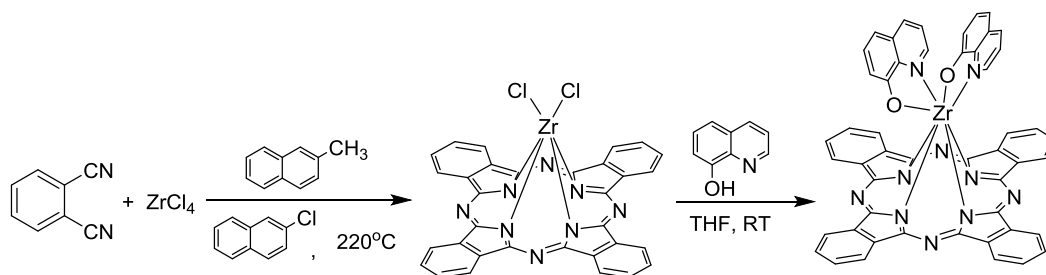
4H), 7.04 (t, 4H), 5.72 (d, 2H). MS (ESI): 913.2 (100%,  $M + 23$ ), 1804.6 (60%,  $2M + 23$ ), 1820.2 (65%,  $2M^+ + 2H_2O$ ).

### 2.3 Structure determination

Crystal data for  $(OQ)_2ZrPc$  were collected using a Rigaku-AFC7 equipped with a Rigaku Saturn CCD area-detector system and multi-layer mirror monochromated  $MoK\alpha$  radiation ( $\lambda = 0.71073 \text{ \AA}$ ) at 173 K under a cold nitrogen stream. The frame data were integrated and absorption correction using a Rigaku CrystalClear program package. All calculations were performed with the SHELXTL-97 program package<sup>[20]</sup>, and the structure was solved by direct methods and refined by full-matrix least-squares against  $F^2$ . All non-hydrogen atoms were refined anisotropically, and hydrogen atoms of organic ligands were generated theoretically onto the specific atoms.

## 3 RESULTS AND DISCUSSION

### 3.1 Synthesis and characterizations



Scheme 1. Synthesis of  $(OQ)_2ZrPc$

The chemical structure of  $(OQ)_2ZrPc$  has been assigned by  $^1H$  NMR, MS and two-dimensional correlation infrared (2D-IR, for details, see the following section) spectroscopy as well as by single-crystal and powder X-ray diffraction analysis. Single crystals of  $(OQ)_2ZrPc$  suitable for X-ray diffraction analyses were obtained by dissolving the pure  $(OQ)_2ZrPc$  in a solvent mixture (THF/ethanol = 90:10 by volume), followed by slow evaporation of the solvents within several days. The obtained crystal has been characterized by single-crystal X-ray analysis at 153 K, which unequivocally confirm the asymmetrically structure of  $(OQ)_2ZrPc$

As deposited in Scheme 1, dichloro  $ZrPc$  ( $Cl_2ZrPc$ ) was prepared according the reported procedure with minor modification<sup>[21,22]</sup>. Due to the high reactive of  $ZrCl_4$ , to avoid the potential hydrolysis, high-boiling solvent 1-chloronaphthalene was used during the synthesis of  $Cl_2ZrPc$ . Moreover, in this step, the addition of 2-methylnaphthalene is to avoid the possible chlorination of benzene ring because the generation of free chlorine radical during the tetramerization of phthalonitrile forms Pc macrocycle, which can be quenched by this easy-chlorinated reagent. The chlorinated 2-methylnaphthalene is easily removed from reaction mixture by filtration and washed with benzene and methanol solvents. Subsequently, the substitution of the two chlorine atoms in  $Cl_2ZrPc$  by 8-hydroxyquinoline resulted in the target compound  $(OQ)_2ZrPc$  in a yield of 62.7%. This isolated complex with additional axial substituents is soluble in most organic solvents (THF, toluene, chloroform and other).

with two deprotonated 8-hydroxyquinoline moieties at one axial side (Fig. 1a). The purity of crystalline materials generated was also investigated by powder X-ray diffraction (Fig. 1b). The later study revealed a single phase for which a good fit between the simulated and observed patterns was observed for  $(OQ)_2ZrPc$ , further confirming its high purity of this unique organic compound.

As shown in Fig. 1a, in each  $(OQ)_2ZrPc$  molecule, the central  $Zr^{4+}$  cation adopts a square antiprism coordination geometry filled by four inner N atoms from one Pc ligand through  $Zr-N$  bonds ( $d_{Zr-N} =$

2.29~2.31 Å), as well as two N and two O atoms from two deprotonated 8-hydroxyquinoline ligands through Zr–N ( $d_{\text{Zr-N}} = 2.40\sim 2.43$  Å) and Zr–O bonds ( $d_{\text{Zr-N}} = 2.11\sim 2.13$  Å), respectively. Due to the bond lengths between  $\text{Zr}^{4+}$  and four inner N atoms of Pc ligand (2.29~2.31 Å) much larger than the half distances between two opposite inner N atoms ( $(3.89\sim 3.91$  Å)/2  $\approx 1.95$  Å), the Pc skeleton adopts a dome-like distortion with the dihedral angles between the opposite isoindole units of 14.87° and 20.29°, respectively. Alternatively, the size of  $\text{Zr}^{4+}$  cation is larger than the inner hole of the four isoindole N atoms of Pc ligand, and thus situated outside the plane of four inner N atoms with a distance of 1.22 Å. Compared to the common Zr–N bonds in the reported ZrPcs ( $d_{\text{Zr-N}} \approx 2.20$

Å)<sup>[23]</sup>, those in this work are slightly increased, which might be attributed to the introduction of 8-oxide quinolone anions at the axial positions, indirectly confirming the impact of the axial ligands on the  $\pi$ -electronic distributions. Also owing to the introduction of axial ligands, the neighboring two Pc molecules are slightly slipped and coupled into Pc pairs through  $\pi\cdots\pi$  interactions with an overlap of only one isoindole unit and a distance of 3.56 Å (Figs. 1c~1d), slightly larger than the thickness value of common aromatic system (*ca.* 3.50 Å)<sup>[22]</sup>. However, in the crystal, the neighboring two Pc pairs are perpendicularly interconnected by weak C–H  $\cdots\pi$  hydrogen bonds to form a three-dimensional structure with voids filled by the disordered THF solvent molecules.

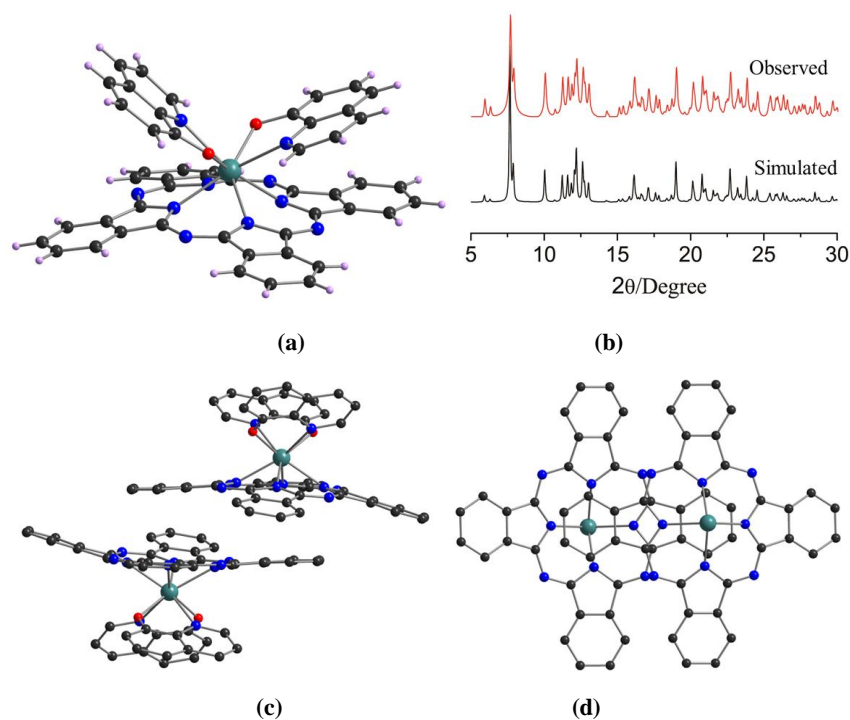


**Fig. 1.** Molecular structure (a) and powder XRD (b) of  $(\text{OQ})_2\text{ZrPc}$ , as well as the close pair of the neighboring two of  $(\text{OQ})_2\text{ZrPc}$  with two different views (c, d). For clarity, H atoms and THF solvent molecules are omitted in (c) and (d), and the two axial 8-oxide quinolone anions are also omitted in (d)

### 3.2 Thermally perturbed 2D-IR correlation spectral properties

The weak intermolecular interactions in the solid-state  $(\text{OQ})_2\text{ZrPc}$  are also reflected in thermally perturbed two-dimensional correlation infrared (2D-IR) spectroscopic studies<sup>[24, 25]</sup>. As shown in Fig. 2, at the low wavenumber region (900~1600

$\text{cm}^{-1}$ ) in the synchronous spectrum (Fig. 2a), three correlations at 1334, 1488, and 1507  $\text{cm}^{-1}$  along the diagonal line in the range of 900~1600  $\text{cm}^{-1}$  were observed, which can be assigned to the stretching and deformation of isoindole moieties of Pc rings, as well as the vibrations of OQ and Pc rings, respectively<sup>[26-28]</sup>. Due to the increased measure

temperature, all these characteristic peaks observed are somewhat shifted to the high-wavenumber region. Moreover, two negative plots at (1334, 1488  $\text{cm}^{-1}$ ) and (1488, 1507  $\text{cm}^{-1}$ ) were observed, indicating that the reverse direction of the intensity variations of peak 1488  $\text{cm}^{-1}$  both to peaks 1334 and 1507  $\text{cm}^{-1}$ . However, in asynchronous spectrum (Fig. 2a), the positive cross-peaks at (1334, 1488  $\text{cm}^{-1}$ ) and (1334, 1507  $\text{cm}^{-1}$ ) have been detected. Considering the intense breathing vibrations for the aromatic rings of OQ but medium for those of Pc at around 1500  $\text{cm}^{-1}$ , those at 1488 and 1507  $\text{cm}^{-1}$  are supposed to be resulted from the vibrations of OQ. Accordingly, these two positive cross-peaks are

ascribed to the thermal perturbation of OQ rings. Similarly, at the high wavenumber region (2600~3400  $\text{cm}^{-1}$ ) in the synchronous spectrum (Fig. 2b), the broad and strong peaks at the ranges of 2800~3000 and 3000~3200  $\text{cm}^{-1}$  indicate the vibration of C-H $\cdots\pi$  hydrogen bonds between THF and the aromatic rings. Considering the weak supramolecular interactions revealed in the single-crystal structure and 2D-IR spectroscopic studies, in order to avoid aggregation, the optical limiting properties of (OQ)<sub>2</sub>ZrPc have been studied in solutions, which is substantiated by the following UV-Vis absorption spectroscopic investigations.

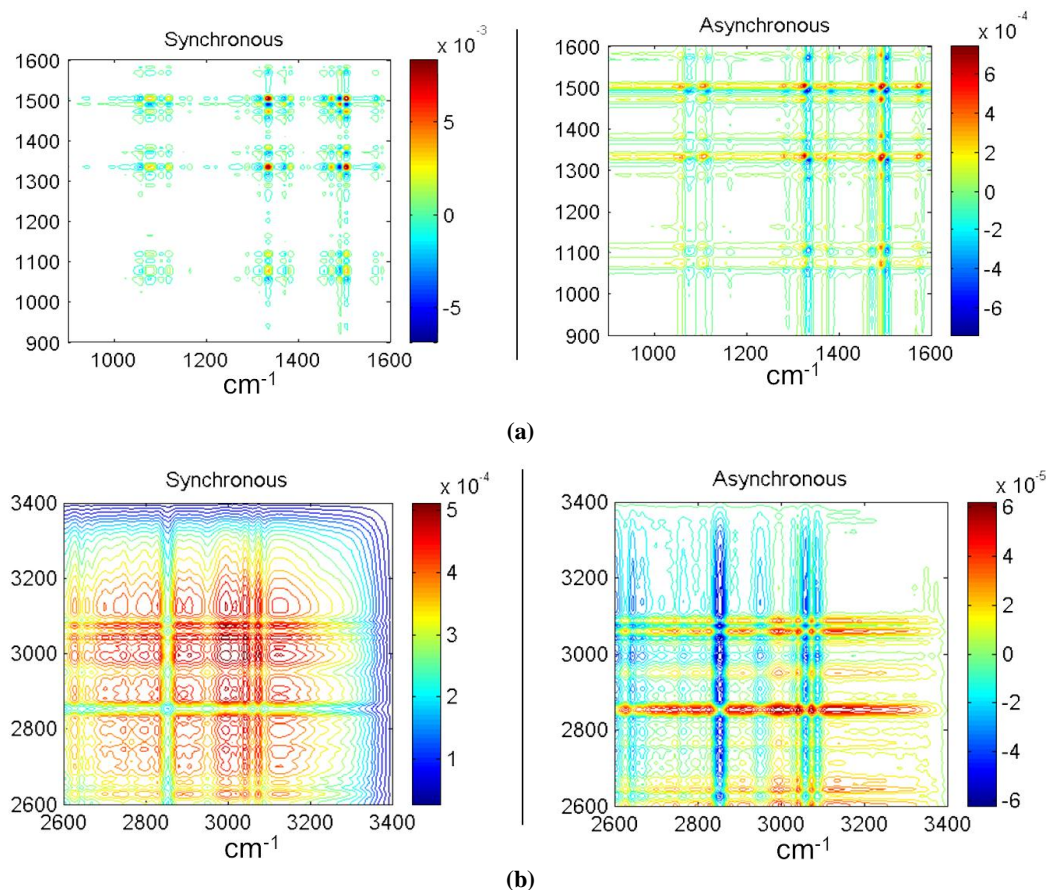


Fig. 2. Thermally perturbed 2D synchronous (left) and asynchronous (right) IR correlation spectra of (OQ)<sub>2</sub>ZrPc at 900~1600  $\text{cm}^{-1}$  (a) and 2600~3400  $\text{cm}^{-1}$  (b) under 50~120 °C

### 3.3 UV-Vis absorption properties

The UV-Vis absorption properties of (OQ)<sub>2</sub>ZrPc have been studied both in dimethylformamide (DMF) and crystalline state. As shown in Fig. 3, in DMF at  $10^{-4}$  mol L<sup>-1</sup>, two pronounced absorption bands, namely the intense Q-band with an absorp-

tion maximum at 682 nm and a shoulder at 615 nm in visible region, as well as B band with an absorption maximum at 345 nm in UV region, were observed, which are assigned to the  $\pi$ - $\pi$  transition of Pcs. Due to the incorporation of two 8-oxide quinoline (OQ) at the axial positions, the absorp-

tion maximum of (OQ)<sub>2</sub>ZrPc is shifted hypsochromically by 2~6 nm in comparison to those of the ZrPc with two chlorine (absorption maximum at *ca.* 688 nm<sup>[9]</sup>) or two  $\beta$ -diketonates at axial positions (absorption maximum at *ca.* 684 nm<sup>[29]</sup>). However, in crystalline state, the absorption maximum of (OQ)<sub>2</sub>ZrPc is 606 nm, which is much blue-shifted in comparison to that in DMF, accompanied by two

shoulder bands at 655 and 735 nm, which are supposed to be attributed to the elimination of solvent effect, as well as the exciton effect evoked from slipped  $\pi$ -stacking of Pc molecules. Compared with these two spectroscopic properties, almost no aggregation species of (OQ)<sub>2</sub>ZrPc were observed in DMF solution of 10<sup>-4</sup> mol L<sup>-1</sup>.

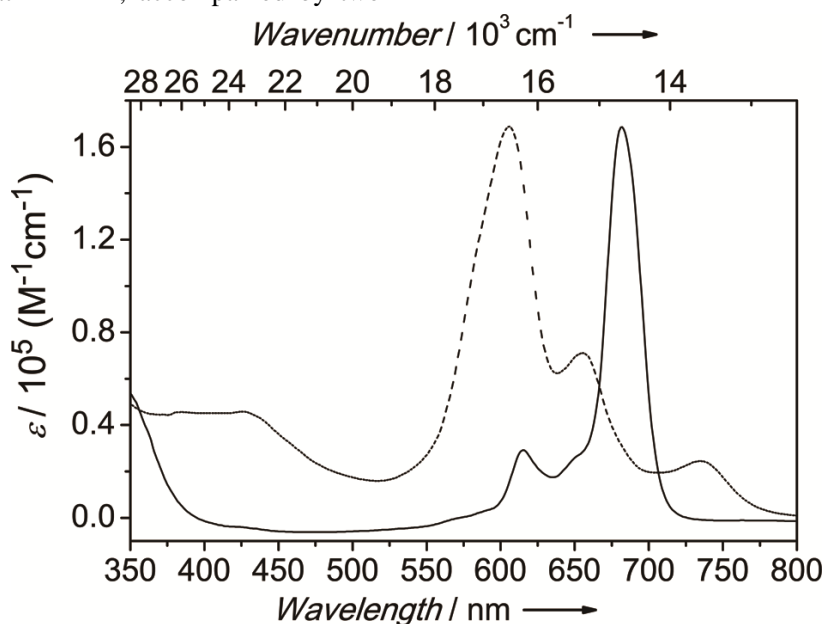
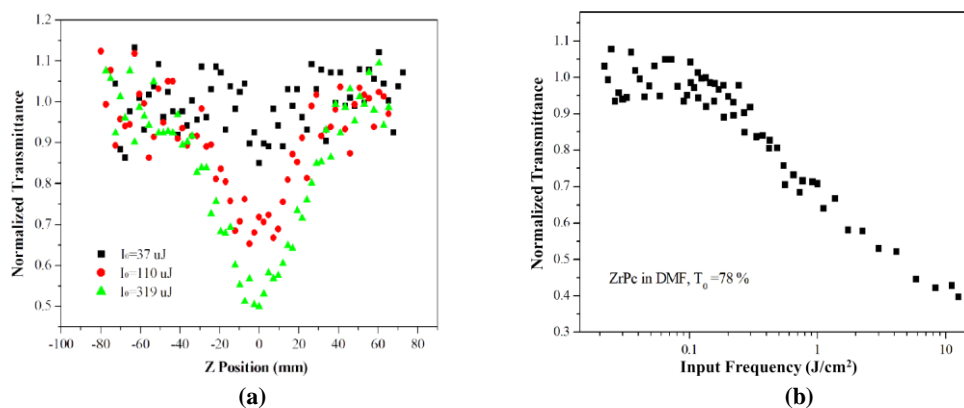


Fig. 3. UV-Vis absorption of (OQ)<sub>2</sub>ZrPc in DMF (solid line, 10<sup>-4</sup> mol L<sup>-1</sup>) and in crystalline state (dashed-dotted line) at room temperature

### 3. 4 Optical limiting properties

Based on the above studies, (OQ)<sub>2</sub>ZrPc is anticipated to be a potential candidate for the optical limiting materials. Thus, a DMF solution of (OQ)<sub>2</sub>ZrPc with a concentration of 10<sup>-4</sup> mol L<sup>-1</sup> has been recorded on the standard open-aperture Z-scan technique using 8 ns Gaussian pulses from a Q-switched Nd:YAG laser at 532 nm, with a pulse repetition rate of 1 Hz. The beam was spatially filtered to remove the higher order modes and focused with a 30 cm focal length lens and the energy of single pulse was 40, 110, 210, 319 and 455  $\mu$ J. As shown in Fig. 4a, the Z-scan profiles of the title compound in the open-aperture configuration exhibit that at each of the excitation energy, the concentrated solution of (OQ)<sub>2</sub>ZrPc shows a decreasing transmission as the focal position is

approached and incident frequency increases, implying that (OQ)<sub>2</sub>ZrPc has a positive nonlinear absorption coefficient, and behaves as a “reverse saturable absorber” for nanosecond pulses at 532 nm. The effective nonlinear absorption coefficient  $\beta$  was estimated to be  $6.69 \times 10^{-14}$  cm/GW, which is close to the common axial substituted metallo-phthalocyanines<sup>[30-32]</sup>. The normalized transmittance of (OQ)<sub>2</sub>ZrPc in DMF versus the input frequency at 532 nm with the linear transmittance of 78% is presented in Fig. 4b, which exhibits the transmittance remains constant at low input frequencies but begins to decrease when the frequency exceeds  $\sim 0.1 \text{ J}\cdot\text{cm}^{-2}$ . This frequency-dependent transmittance feature is a typical optical limiting response.



**Fig. 4.** Typical open aperture Z-scan traces of the DMF solution of  $(\text{OQ})_2\text{ZrPc}$  ( $10^{-4}$  mol  $\text{L}^{-1}$ ) with a pulse intensity of  $I_0 = 37, 110,$  and  $319$  uJ at  $532$  nm (a) and its normalized transmittance as a function of the input frequency at  $532$  nm (b)

## 4 CONCLUSION

In summary, we have reported a novel ZrPc bearing two 8-oxide quinoline anions at the same axial side. Due to the introduction of two 8-oxide quinolone anions at the axial positions, the nonlinear optical properties of this unique complex

studied by the open aperture Z-scan and normalized transmittance showed that it possessed a moderately effective nonlinear absorption coefficient  $\beta_{\text{eff}}$  of  $6.69 \times 10^{-14}$  cm/GW at  $532$  nm in DMF solution, implying it is a promising candidate for optical limiting materials.

## REFERENCES

- (1) Nalwa, H. S. Organic materials for nonlinear optics. *Adv. Mater.* **1993**, 5, 341–358.
- (2) Bredas, J. L.; Adant, C.; Tackx, P.; Persoons, A. Third-order nonlinear optical response in organic materials: theoretical and experimental aspects. *Chem. Rev.* **1994**, 94, 243–278.
- (3) Spangler, C. W. Recent development in the design of organic materials for optical power limiting. *J. Mater. Chem.* **1999**, 9, 2013–2020.
- (4) Smilowitz, L.; McBranch, D.; Klimov, V.; Robinson, J. M.; Koskelo, A.; Grigorova, M.; Mattes, B. R.; Wang, H.; Wudl, F. Enhanced optical limiting in derivatized fullerenes. *Opt. Lett.* **1996**, 21, 922–924.
- (5) Sun, Y. P.; Riggs, J. E.; Liu, B. Optical limiting properties of [60]fullerene derivatives. *Chem. Mater.* **1997**, 9, 1268–1272.
- (6) Tutt, L. W.; Boggess, T. F. A review of optical limiting mechanisms and devices using organics, fullerenes, semiconductors and other materials. *Prog. Quant. Electron.* **1993**, 17, 299–338.
- (7) Liu, Z. B.; Tian, J. G.; Guo, Z.; Ren, D. M.; Du, F.; Zheng, J. Y.; Chen, Y. S. Enhanced optical limiting effects in porphyrin-covalently functionalized single-walled carbon nanotubes. *Adv. Mater.* **2008**, 20, 511–515.
- (8) Calvete, M.; Yang, G. Y.; Hanack, M. Porphyrins and phthalocyanines as materials for optical limiting. *Syn. Met.* **2004**, 141, 231–243.
- (9) Du, Y.; Dong, N.; Zhang, M.; Zhu, K.; Na, R.; Zhang, S.; Sun, N.; Wang, G.; Wang, J. Covalent functionalization of graphene oxide with porphyrin and porphyrin incorporated polymers for optical limiting. *Phys. Chem. Chem. Phys.* **2017**, 19, 2252–2260.
- (10) Hanack, M.; Schneider, T.; Barthel, M.; Shirk, J. S.; Flom, S. R.; Pong, R. G. S. Indium phthalocyanines and naphthalocyanines for optical limiting. *Coord. Chem. Rev.* **2001**, 219, 235–258.
- (11) Chen, Y.; Hanack, M.; Arakic, Y.; Ito, O. Axially modified gallium phthalocyanines and naphthalocyanines for optical limiting. *Chem. Soc. Rev.* **2005**, 34, 517–529.
- (12) Chen, Y.; Gao, L.; Feng, M.; Gu, L.; He, N.; Wang, J.; Araki, Y.; Blau, W. J.; Ito, O. Photophysical and optical limiting properties of axially modified phthalocyanines. *Mini-Rev. Org. Chem.* **2009**, 6, 55–65.
- (13) Dini, D.; Calvete, J. F. M.; Hanack, M. Nonlinear optical materials for the smart filtering of optical radiation. *Chem. Rev.* **2016**, 116, 13043–13233.
- (14) Shirk, J. S.; Pong, R. G. S.; Bartoli, F. J.; Snow, A. W. Optical limiter using a lead phthalocyanine. *Appl. Phys. Lett.* **1993**, 63, 1880–1882.
- (15) Shirk, J. S.; Pong, R. G. S.; Flom, S. R.; Bartoli, F. J.; Boyle, M. E.; Snow, A. W. Lead phthalocyanine reverse saturable absorption optical limiters.

*Pure Appl. Opt.* **1996**, 5, 701–707.

- (16) Managa, M.; Khene, S.; Britton, J.; Martynov, A. G.; Gorbunova, Y. G.; Tsivadze, A. Y.; Nyokong, T. Photophysics and NLO properties of Ga(III) and In(III) phthalocyanines bearing diethyleneglycol chains. *J. Porphyr. Phthalocya* **2018**, 22, 137–148.
- (17) Wang, T.; Wang, X.; Zhang, J.; Wang, C.; Shao, J.; Jiang, Z.; Zhang, Y. Synthesis, structure and third-order optical nonlinearities of hyperbranched metal phthalocyanines containing imide units. *Dyes Pigments* **2018**, 154, 75–81.
- (18) Perry, J. W.; Mansour, K.; Lee, I. Y. S.; Wu, X. L.; Bedworth, P. V.; Chen, C. T.; Ng, D.; Marder, S. R.; Miles, P.; Wada, T.; Tian, M.; Sasabe, H. Organic optical limiter with a strong nonlinear absorptive response. *Science* **1996**, 273, 1533–1536.
- (19) Shirik, J. S.; Pong, R. G. S.; Flom, S. R.; Heckmann, H.; Hanack, M. Effect of axial substitution on the optical limiting properties of indium phthalocyanines. *J. Phys. Chem. A* **2000**, 104, 1438–1449.
- (20) Sheldrick, G. M. *SHELXS-97, Program for X-ray Crystal Structure Solution*. University of Göttingen, Germany **1997**.
- (21) Tomachynski, L. A.; Tretyakova, I. N.; Chernii, V. Y.; Volkov, S. V.; Kowalska, M.; Legendziewicz, J.; Gerasymchuk, Y. S.; Radzki, S. Synthesis and spectral properties of Zr(IV) and Hf(IV) phthalocyanines with  $\beta$ -diketonates as axial ligands. *Inorg. Chim. Acta* **2008**, 361, 2569–2581.
- (22) Gorsch, M.; Franken, A.; Sievertsen, S.; Homborg, H. Zirconiumphthalocyanine: darstellung und eigenschaften chloridhaltiger phthalocyanine des drei- und vierwertigen zirconiums; kristallstruktur von *cis*-di(triphenylphosphin)iminium-tri(chloro)phthalocyaninato(2-)-zirconat(IV)-di(dichlormethan). *Z. Anorg. Allg. Chem.* **1995**, 621, 607–616.
- (23) Hunter, C. A.; Sanders, J. K. M. The nature of  $\pi$ - $\pi$  interactions. *J. Am. Chem. Soc.* **1990**, 112, 5525–5534.
- (24) Chen, Y.; Shen, X.; Zhang, H.; Huang, C.; Cao, Y.; Sun, R. The structure and two-dimensional correlation infrared spectroscopy study of a new 2D polyoxomolybdate complex containing  $\beta$ -octamolybdate linked up by potassium ions:  $(4,4'$ -Hbpy) $_2$ (K $_2$ Mo $_8$ O $_{26}$ ). *Vib. Spectrosc.* **2006**, 40, 142–147.
- (25) Chen, Y.; Zhang, H.; Wang, X.; Huang, C.; Cao, Y.; Sun, R. Structure and two-dimensional correlation infrared spectroscopy study of two isomeric forms of the octamolybdate cluster. *J. Solid State Chem.* **2006**, 179, 1674–1680.
- (26) Zhang, X.; Zhang, Y.; Jiang, J. Towards clarifying the N–M vibrational nature of metallo-phthalocyanines: infrared spectrum of phthalocyanine magnesium complex: density functional calculations. *Spectrochim. Acta A* **2004**, 60, 2195–2200.
- (27) Jiang, J.; Arnold, D. P.; Yu, H. Infra-red spectra of phthalocyanine and naphthalocyanine in sandwich-type (na)phthalocyaninato and porphyrinato rare earth complexes. *Polyhedron* **1999**, 18, 2129–2139.
- (28) Arıcı, K.; Yurdakul, M.; Yurdakul, S. HF and DFT studies of the structure and vibrational spectra of 8-hydroxyquinoline and its mercury(II) halide complexes. *Spectrochim. Acta A* **2005**, 61, 37–43.
- (29) Chernii, V. Y.; Bon, V. V.; Tretyakova, I. N.; Severinovskaya, O. V.; Volkov, S. V. Novel zirconium(IV) and hafnium(IV) phthalocyanines with dibenzoylmethane as out-of-plane ligand: Synthesis, X-ray structure and fluorescent properties. *Dyes Pigments* **2012**, 94, 187–194.
- (30) O'Flaherty, S. M.; Hold, S. V.; Cook, M. J.; Torres, T.; Chen, Y.; Hanack, M.; Blau, W. J. Molecular engineering of peripherally and axially modified phthalocyanines for optical limiting and nonlinear optics. *Adv. Mater.* **2003**, 15, 19–32.
- (31) Chen, Y.; Fujitsuka, M.; O'Flaherty, S. M.; Hanack, M.; Ito, O.; Blau, W. J. Strong optical limiting of soluble axially substituted gallium and indium phthalocyanines. *Adv. Mater.* **2003**, 15, 899–902.
- (32) Chen, Y.; O'Flaherty, S.; Fujitsuka, M.; Hanack, M.; Subramanian, L. R.; Ito, O.; Blau, W. J. Synthesis, characterization, and optical-limiting properties of axially substituted gallium(III) naphthalocyanines. *Chem. Mater.* **2002**, 14, 5163–5168.